PERGAMON

International Journal of Solids and Structures 39 (2002) 4605–4614

INTERNATIONAL JOURNAL OF SOLIDS and STRUCTURES

www.elsevier.com/locate/ijsolstr

Elasticity of DLCA model gels with loops

Hang-Shing Ma [a,*], Jean-H. Prévost [b], George W. Scherer [c]

[a] *Department of Chemical Engineering, Princeton University, Princeton, NJ 08544, USA*

[b] *Department of Civil and Environmental Engineering, Princeton University, Princeton, NJ 08544, USA*

[c] *Department of Civil and Environmental Engineering & Princeton Materials Institute, Princeton University, Princeton, NJ 08544, USA*

Received 8 April 2002; received in revised form 20 May 2002

Abstract

Aggregation is a common natural phenomenon, but the structure–property relationship of the resulting porous, fractal gels is not well understood. An earlier study using the diffusion-limited cluster–cluster aggregation model revealed that loop structure is lacking in the model gels to account for their mechanical properties. The dangling bond deflection model was then developed to address loop formation during the aggregation process. This article describes the finite element method implemented to measure the various moduli of the resulting gel structure, which was modeled as a network of linearly elastic beams. The well-known empirical correlation in gels—the power–law scaling of Young's modulus with relative densities—was reproduced, and the scaling exponent of about 3.6, which is consistent with the experimental results, was captured in the analysis. About 70% of the total strain energy in the network came from bending of the beams. The contrast in the scaling exponent as compared to the open-cell foam model is attributed to the change of connectivity in the gel network when the density of the aggregate is adjusted.

Keywords: Aerogel; Sol–gel; Diffusion-limited cluster–cluster aggregation with dangling bond deflection; Finite element method; Elasticity; Beam theory; Fractal; Modulus–density scaling

1. Introduction

Fractal gels, in the form of mesoporous, random aggregates (Brinker and Scherer, 1990), can be found in a number of naturally occurring materials, biological systems and commercial products, e.g., aerosol, alginate, thin films, low-k interlayer dielectric, controlled release drug delivery system, thermal insulation panels and aerogels (Hrubesh, 1998). However, they are notorious for their poor mechanical properties when processing and handling are concerned in practical applications. There is a lack of understanding of the mechanical structure–property relationship of these porous structures, owing to difficulties in characterizing them by experiments. What is known though is the scaling relationship between the Young's moduli E of these high-porosity gels and their relative densities ρ,

* Corresponding author. Tel.: +1-609-258-4704; fax: +1-609-258-1563.
E-mail address: hangma@princeton.edu (H.-S. Ma).

0020-7683/02/$ - see front matter
PII: S0020-7683(02)00382-7

$$E \propto \rho^m, \tag{1}$$

with a large exponent m, usually between 3 and 4 (Woignier et al., 1989; Pekala et al., 1991; Gross et al., 1993; Scherer et al., 1995a). Their compliant nature, especially towards the lower density, makes them highly susceptible to deformation during characterization and hence gives erroneous results (Scherer et al., 1995b). The network stiffness depends on connectivity and there is not any experimental technique that can quantify the connectivity of a random structure.

We attempted to study the mechanical structure–property relationship of gels by computer modeling, using the diffusion-limited cluster–cluster aggregation (DLCA) model (Meakin, 1983; Kolb et al., 1983) to simulate the gel growth, and then the finite element method to evaluate the elastic bulk modulus K of the resulting structure (Ma et al., 2000). The DLCA model creates too little loop structure and too many dangling branches to account for the network stiffness. In reality, these fluffy dangling branches are subjected to thermal excitation during which contacts between them can lead to formation of new bonds and loops. In fact, such phenomenon is the cause of syneresis in the aging of gels (Brinker and Scherer, 1990). The fluctuations of these flexible branches were modeled as random rotational motions, and the model was implemented in the DLCA which, as a whole, is termed as the DLCA with dangling bond deflection (DLCADEF). This improved model is capable of creating loops in the network. The objective of this study is to illustrate the linear elastic properties of these DLCADEF networks, using finite element method. The results show agreement with the experimental scaling relationship of gels as illustrated by Eq. (1).

2. Constraints on modeling

2.1. Modeling of sol–gel transition

The model gel networks were simulated by the DLCADEF model, developed by Ma et al. (2002). The model is based on the off-lattice version of the DLCA in a cubic box with periodic boundary conditions (Hasmy et al., 1994). For the silicate solution, the primary particles in the DLCA model represent the polycyclic oligomers derived from the molecular precursors with acidic catalysis or neutral condition, or dense colloidal particles with base catalysis (Devreux et al., 1990; Vacher et al., 1988). The originality of the DLCADEF model is the modeling of the fluctuations of the dangling bonds and their associated dangling branches as random deflection motions. Deflection of dangling branches creates loops in the network when these branches make contact and form bonds with the other parts of the network. These loops provide stiffness to the network, and continue to form during both the gelation and aging processes until a negligible amount of dangling branches is left. The relative density ρ of a model gel network is determined by

$$\rho = \frac{(\pi/6)n_{\mathrm{p}}}{b^3}, \tag{2}$$

where n_{p} is the number of spherical particles of unit diameter in cubic box of length b (in units of particle size). The values of ρ studied include 0.018, 0.03, 0.056, 0.1 and 0.18, which span an order of magnitude. The bond compliance factor F, which adjusts the frequency of deflections of dangling bonds relative to Brownian displacements of clusters, is investigated at levels of 10, 100 and 1000. The model gel networks are generated at various b to determine the minimum size at each density beyond which the results become size-invariant. Moreover, five realizations of the model were generated at each combination of ρ, F and b for statistical confidence of the results.

2.2. Modeling of network deformation

The DLCADEF model creates a gel network in the form of a single aggregate of interconnected particles in a box. The stiffness of the network is provided by the rigidity of the interparticle bonds and the connectivity of the particles. Each interparticle bond is assumed to behave as a beam element, which is a straight, linearly elastic bar of uniform cross section and unit length, capable of resisting axial and shear forces, and also bending and twisting moments (Przemieniecki, 1985). The node at each end of a beam then represents the center of the particle constituting the bond. The constitutive equation describing the deformation of a beam can be written in the form of a force-displacement relationship,

$$\underline{\mathbf{s}} = \underline{\underline{\mathbf{c}}} \cdot \underline{\mathbf{u}}, \tag{3}$$

where $\underline{\underline{\mathbf{c}}}$, $\underline{\mathbf{u}}$ and $\underline{\mathbf{s}}$ are the local stiffness matrix, local displacement vector and local force vector respectively (Przemieniecki, 1985). The vector $\underline{\mathbf{u}}$ is a 12-element vector containing the axial displacements and rotations about the three orthogonal axes at both ends of the beam. The vector $\underline{\mathbf{s}}$ carries the forces and moments of the corresponding twelve degrees of freedom of movement. The matrix $\underline{\underline{\mathbf{c}}}$ is a 12×12 matrix containing the geometrical and elasticity information of the beam, including the Young's modulus, Poisson's ratio, moment of inertia and radius. The Young's modulus of the beams is chosen to be 100,000 arbitrary units with zero Poisson's ratio, and the radius to be 0.2 in units of particle size. The choice of these values, as will be shown later, does not affect the conclusion of the analysis.

Some of the bonds in the model gel pass through the box enclosing the network and reenter at the opposite side in compliance with the periodic boundary conditions. The six faces of the box can be represented by planes of $x = 0$, $y = 0$, $z = 0$, $x = b$, $y = b$ and $z = b$, where x, y, z are the three orthogonal directions constituting the edges of the box. Suppose particles A and B share a bond, denoted as AB, through the periodic boundary, and are adjacent to the plane $x = 0$ and b respectively. An imaginary particle A_p is created adjacent to the plane $x = b$ such that A and A_p are exactly equivalent in terms of periodicity, but are at a distance b apart in the x-direction and A_p is directly bonded to B as $A_\mathrm{p}B$. Imaginary particles like A_p are created adjacent to the planes $x = b$, $y = b$ and $z = b$ in conjunction with the particles like A so that all the cross-boundary bonds like AB are then replaced by normal bonds like $A_\mathrm{p}B$ and equivalent pairs like (A, A_p). These equivalent pairs represent the periodic particle boundary of the network that will be needed for imposing the boundary condition of deformation.

Hydrostatic compression of the network is modeled by displacing both the real and imaginary particles in every equivalent pair normal to their boundary plane and towards each other. Therefore in the case of the pair (A, A_p), A is pushed towards the $+x$ direction while A_p towards the $-x$ direction. The distance u_K displaced for each boundary particle is given by

$$u_\mathrm{K} = \frac{b}{2}\left(1 - \sqrt[3]{1 + \varepsilon_\mathrm{V}}\right), \tag{4}$$

where ε_V is the engineering volumetric strain and is arbitrarily chosen to be -1%. In addition to the prescribed displacement, the other five degrees of freedom of the particles in each equivalent pair are constrained to move exactly in phase with the respective ones of the imaginary particle. That means the displacements in y, z, the torsion in x, and the bending rotations in y, z directions of A and A_p are the same after the compression. The pairs like (A, A_p) are described as slaved nodes for the remaining five non-prescribed degrees of freedom.

Such a boundary condition for compression is not strictly periodic, because the reaction forces experienced by the boundary particles in any equivalent pair are not constrained to be the same. Therefore, there may be some artificial deformation at the boundary which does not represent the true strain. Large models and repetitions become necessary to minimize the boundary effect. Moreover, since the model gel network is truly periodic, the boundary of the enclosing box can be placed anywhere inside the infinite

structure. Therefore, further statistical confidence can be achieved by shifting the box to different positions of the infinite network and measuring the network moduli of the corresponding configurations. Eight measurements were taken from each realization of the model gel network, by shifting the boundary with the displacements in the (x,y,z) direction of $(0,0,0)$, $(0.5b,0,0)$, $(0,0.5b,0)$, $(0,0,0.5b)$, $(0.5b,0.5b,0)$, $(0.5b,0,0.5b)$, $(0,0.5b,0.5b)$ and $(0.5b,0.5b,0.5b)$. With five realizations at each model configuration, a total of forty measurement could be made.

The calculation of the response of the network under compression was performed by the finite element method using the program called Dynaflow®, originated by Prévost (1983). The constitutive equation of deforming a beam, represented by Eq. (3), is spatially transformed for each beam from its local coordinate to the datum coordinate system sustained by the orientation of the box (Przemieniecki, 1985), so as to take into account the different orientations of the beams. Then, the transformed local stiffness matrices are assembled according to the connectivity of the beams into a global stiffness matrix $\underline{\underline{\mathbf{C}}}$, from which a global force–displacement relationship can be written as

$$\underline{\mathbf{S}} = \underline{\underline{\mathbf{C}}} \cdot \underline{\mathbf{U}}, \tag{5}$$

where $\underline{\mathbf{S}}$ and $\underline{\mathbf{U}}$ are the global displacement and force vectors respectively (Hughes, 1987), and contain the full six degrees of freedom of displacements, rotations, forces and moments of each node in the network with reference to the datum coordinate. The prescribed boundary conditions of displacement and the slave conditions of the boundary nodes are incorporated in the matrix Eq. (5). The unknown elements in $\underline{\mathbf{S}}$ and $\underline{\mathbf{U}}$ of the beams are solved from Eq. (5) by Choleski factorization of $\underline{\underline{\mathbf{C}}}$, with minimum degree of ordering and sparse matrix storage (Duff et al., 1989), and then Gaussian elmination. The calculation does not consider beam breaking or node congestion because they should be dominant only in the plasticity regime (i.e., at large strain), which is beyond the scope of this study.

The modulus of the network can be evaluated from $\underline{\mathbf{S}}$ and $\underline{\mathbf{U}}$ of the finite element analysis. There are two methods to calculate the modulus: one uses the reaction forces of the boundary particles associated with the prescribed displacement boundary conditions. The total reaction force normal to one face of the network is equal to and counterbalance the opposite side of the network as a criterion for mechanical equilibrium, and to ensure the boundary conditions are homogeneous such that there are not any rigid body motions. Assuming that the total reaction force at one side of the network in the x, y and z directions are S_x, S_y and S_z respectively. In the case of hydrostatic compression when the values of S_x, S_y and S_z are fairly close to each other, the bulk modulus K of the network can be evaluated by

$$K = \frac{S_x + S_y + S_z}{3b^2\varepsilon_{\mathrm{V}}}. \tag{6}$$

The method used in this study is based on the strain energy approach. The total strain energy φ absorbed by the network from the compression is defined by

$$\varphi = \frac{1}{2}(\underline{\mathbf{S}}^t \cdot \underline{\mathbf{U}}). \tag{7}$$

The bulk modulus K of the network can be evaluated by

$$K = \frac{2}{\varepsilon_{\mathrm{V}}^2 b^3}\varphi. \tag{8}$$

Longitudinal compression is modeled in a way similar to that of hydrostatic compression, except that only the particles adjacent to one of the three pairs of the parallel planes are displaced. The displacement u_x is given by

$$u_x = \frac{b\varepsilon_x}{2}, \tag{9}$$

where ε_x is the engineering uniaxial strain. Boundary particles at the other faces are held at zero displacement normal to their respective planes. All the equivalent pairs are slaved for the non-prescribed five degrees of freedom of movement. The longitudinal modulus H_x is given by

$$H_x = \frac{2}{\varepsilon_x^2 b^3}\varphi, \tag{10}$$

with φ calculated in the same way as Eq. (7) but under the longitudinal compression boundary conditions. The resultant H, or c_{11} can be derived from the arithmetic mean of H_x, H_y and H_z, with the latter two evaluated in the same way as H_x but by compressing in the y and z direction respectively.

The Poisson's ratio v_p can be derived to be

$$v_p = \frac{3K - H}{3K + H}, \tag{11}$$

which is evaluated for each individual realization of the model gel network. The Young's modulus E of the network is related to K and v_p by (Timoshenko and Goodier, 1970)

$$E = 3K(1 - 2v_p). \tag{12}$$

3. Results

3.1. Effect of parameters

The dependence of K of the DLCADEF model gel networks on b was analyzed by observing the trend of the former against the reciprocal of the latter. Fig. 1 shows the results for models of $F = 100$ and ρ between 0.018 and 0.18. The ultimate size independent value of K should in principle be obtained at $b^{-1} \to 0$ that represents infinite box size. While this is computationally impractical, the average value of K at each ρ converges to a certain value and its confidence interval narrows down as b increases. From the convergence

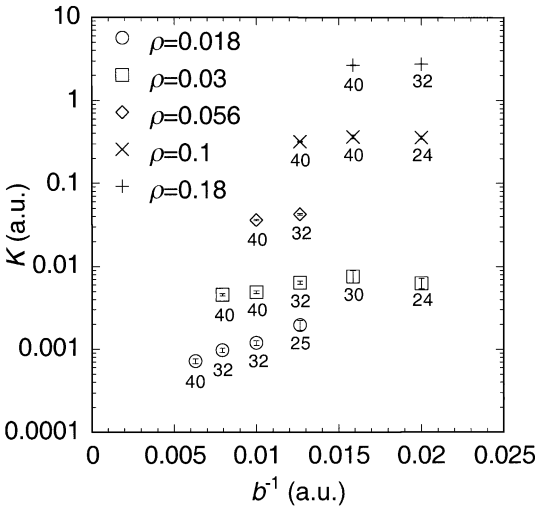

Fig. 1. Effect of network size b on bulk modulus K for DLCADEF networks of bond compliance factor $F = 100$ and various densities ρ (the number underneath the symbols denote the total number of samples).

trends, we conclude that the average K of $\rho = 0.03$, 0.056, 0.1 and 0.18 have reached the size-independent value at $b = 126$, 100, 79 and 63 respectively, while that of $\rho = 0.018$ has not leveled off for the available sizes. The same conclusions were drawn for $F = 10$ and 1000 and for H. All the subsequent analyses are performed based on these size-invariant results.

The modulus of the network is linearly proportional to the Young's modulus of the beam, and scales with the radius of the beam with an exponent of about 4. With up to forty measurements on each model configuration, the standard errors are found negligible for the data in the subsequent analysis. The value of strain has no effect on the calculated modulus, as expected from the linear elasticity formulation.

3.2. Linear elasticity

The size-invariant bulk moduli K of the DLCADEF model gel networks are plotted against their relative densities ρ on the log–log scale in Fig. 2. The data demonstrate a power–law relationship,

$$K \propto \rho^{m_K}, \tag{13}$$

with the exponent m_K increasing from 3.5 to 3.7 as the bond compliance factor F increases from 10 to 1000. The modulus is insensitive to F when compared to its dependence on ρ. The same scaling relationship as Eq. (13) exists for the longitudinal modulus H, although the scaling exponents, defined as m_H are slightly different. The data for networks of $\rho = 0.018$ and $b = 159$ are shown in Fig. 2 for illustration only and are not involved in the least square fitting. However, the quality of the fit and the exponents would only be slightly affected even if these size-dependent data were included.

The dependence of the Poisson's ratio v_p with ρ and F of the DLCADEF model is presented in Fig. 3. The Poisson's ratio increases from 0.125 ± 0.01 at $\rho = 0.03$, to 0.145 ± 0.01 at $\rho = 0.18$. Within the statistical error, v_p is higher with larger F. The scaling of the Young's modulus E of the network with ρ is shown in Fig. 4. The scaling exponents of K, H and E versus ρ at various F are tabulated in Table 1, showing that the exponents are always about 3.6 ± 0.2.

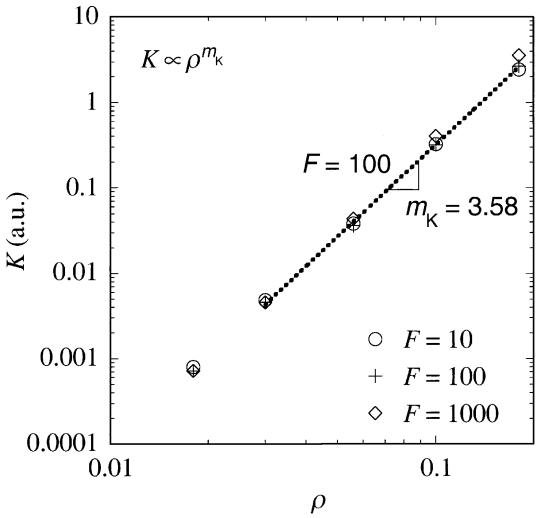

Fig. 2. Scaling of bulk modulus K with relative density ρ at various bond compliance factor F of the DLCADEF networks (data of $\rho = 0.018$ are for illustration only; regression shows $m_K = 3.58$ for data of $F = 100$).

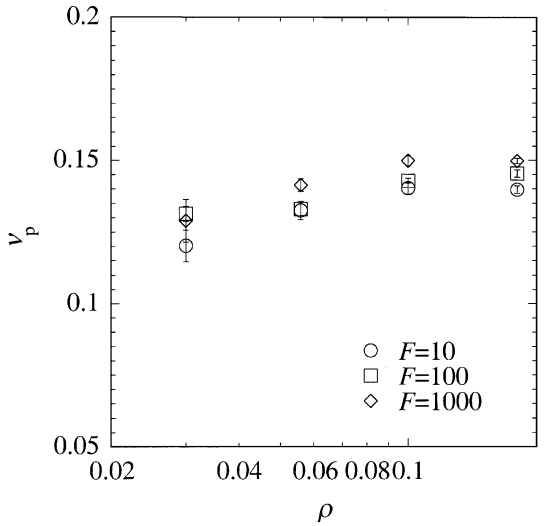

Fig. 3. Dependence of Poisson's ratio ν_p on relative density ρ at various bond compliance factor F of the DLCADEF networks.

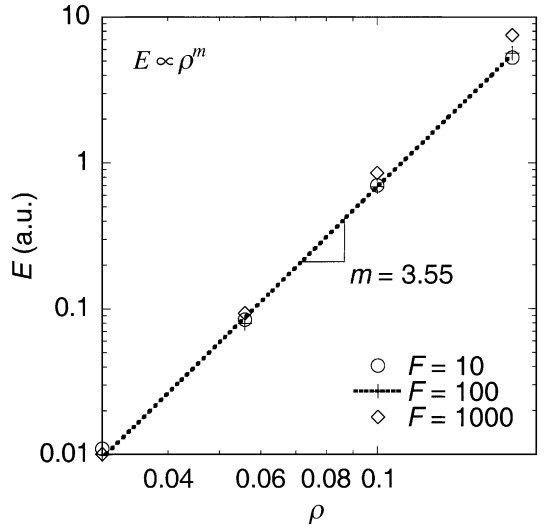

Fig. 4. Scaling of Young's modulus E with relative density ρ at various bond compliant factor F of the DLCADEF networks (regression shows $m = 3.55$ for data of $F = 100$).

Table 1
Scaling exponents of modulus-density relationships for DLCADEF model gels of various bond compliance factor F under different forms of deformation

F	m_K	m_H	m
10	3.49	3.47	3.46
100	3.58	3.56	3.55
1000	3.73	3.71	3.70

3.3. Mode of deformation

The three-dimensional modeling of hydrostatic compression is illustrated by a two-dimensional DLCADEF model gel network, unstrained in Fig. 5(a) and compressed in Fig. 5(b). The network is represented by connections of nodes (particle centers) with beams (bonds). A breakdown of the different modes of deformation contributing to the total strain energy of the network is depicted in Fig. 6. Bending is the major mode of deformation of the network, accounting for $70\% \pm 1\%$ of the total strain energy for the various ρ and F studied. Uniaxial compression or extension of the beam contributes less than 2% to the total.

4. Analysis

The model gel networks simulated by the DLCADEF model exhibit the same modulus–density scaling relationship as aerogels and other high-porosity random aggregate materials, with a similar scaling exponent of about 3.6. The Poisson's ratio is also similar for both gels from modeling and experiment (Gross et al., 1988; Scherer, 1992). As a result, the DLCADEF model is capable of capturing altogether the growth kinetics, structure (Ma et al., 2002) and the mechanical properties of the real systems. To the knowledge of the authors, no other model gel networks have demonstrated such resemblance. The reproduction of the scaling relationship stems from the distinctive structural features and connectivity of the DLCADEF networks which resemble the real gels.

The parameters assumed in the finite element analysis, including the strain, the radius and Young's modulus of beams, have no effect on the scaling exponents. The linear relationship between the modulus of the network and the Young's modulus of the beam is a direct consequence of the linear elasticity of the beams, and the fourth-power relationship of the radius of the beam to the network modulus originates from bending of the beams (Timoshenko and Goodier, 1970), which is the dominant mode of deformation in the

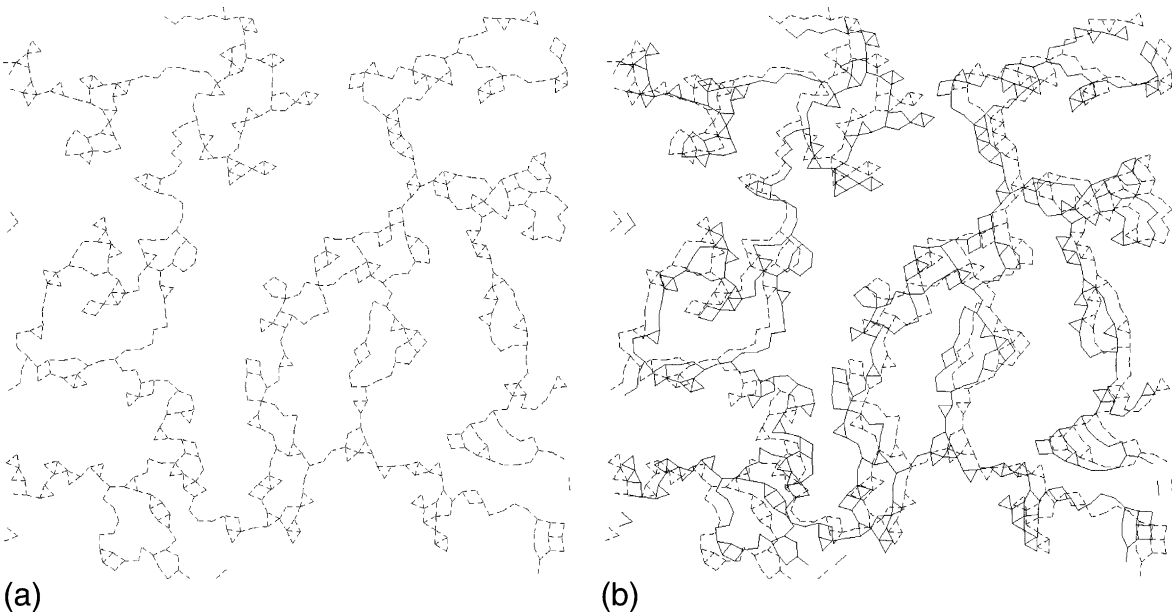

Fig. 5. (a) Two-dimensional DLCADEF network (node represents particle and link represents bond), (b) with solid line representing compressed state and broken line representing unstrained state.

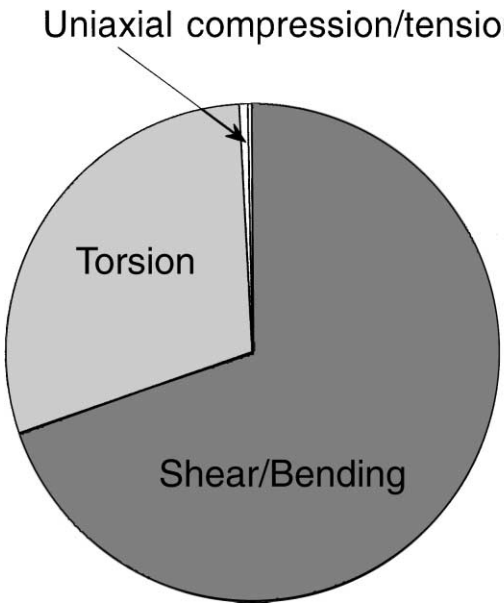

Fig. 6. Contribution of different modes of deformation of the beams to the total strain energy (and modulus) of the DLCADEF network.

network. They vary the modulus to the same extent at any density, so that they are insensitive to the scaling exponents. This is understandable because the beam parameters, which correspond to the physical properties of the interparticle bonds in real gels, should indeed be independent of the concentration or density in the sol–gel process. The strain applied on the network, as expected, does not affect the scaling relationship or exponent because of the linear elasticity formulation and the absence of plasticity assumptions (i.e., no bond breaking or particle congestion). Therefore the present scheme is not appropriate for studying yielding and compression hardening of gels.

Shear deformation, or bending of the beams, is the major mode of deformation in the network. This agrees with the assumption of the open-cell foam model (Gibson and Ashby, 1997), but that model yields the exponent $m = 2$, far smaller than the ones found from the DLCADEF networks and the real gels. A big difference between the two models is that the open-cell foam assumes its density varies quadratically with the aspect ratio of the beam, while the DLCADEF model has beams at a constant aspect ratio at all densities. Some cellular materials, like microcellular polymer and glass foam, have their densities adjusted by manipulating the thickness of the beams in the processing. However, for the sol–gel process, the gel density is controlled by the concentration of precursors or colloidal particles. Aggregation creates structures with varying connectivity but the same kind of bonds at different densities, rather than the same structure with different feature size (e.g. beam thickness) in open-cell foams. While the open cell foam model is not applicable in this context, the mechanical structure–property relationship of fractal gels is explained by Ma and co-workers (2001, in preparation).

5. Conclusion

The model gel network, simulated by the DLCADEF model, captures the linear elastic properties exhibited by real gels and porous aggregates: it reproduces the characteristic modulus–density scaling

relationship in the form of Eq. (1) with the correct exponent m of about 3.6. Bending of the beams is the major mode of deformation when the network is under strain. However, unlike polymer or ceramic foams, the density variation of the gels is accompanied by significant change in connectivity due to the nature of the aggregation process. Therefore the scaling exponent m is much higher than the value ($m = 2$) predicted by the open-cell foam model.

Acknowledgements

The financial support for the study of the mechanical structure–property relationship of aerogels is provided by Department of Energy Research Contract (DOE DEFG02-97ER45642). The authors would like to thank Rémi Jullien for the idea of the DLCADEF model.

References

Brinker, C.J., Scherer, G.W., 1990. Sol–Gel Science. Academic Press, New York.

Devreux, F., Boilot, J.P., Chaput, F., Lecomte, A., 1990. Sol–gel condensation of rapidly hydrolyzed silicon alkoxides—a joint ^{29}Si NMR and small-angle X-ray scattering study. Physical Review A 41, 6901.

Duff, I.S., Erisman, A.M., Reid, J.K., 1989. Direct Methods for Sparse Matrices. Oxford University Press, New York.

Gibson, L.J., Ashby, M.F., 1997. Cellular Solids: Structure and Properties, second ed. Cambridge University Press, UK.

Gross, J., Reichenauer, G., Fricke, J., 1988. Mechanical properties of SiO_2 aerogels. Journal of Physics D: Applied Physics 21, 1447.

Gross, J., Schlief, T., Fricke, J., 1993. Ultrasonic evaluation of elastic properties of silica aerogels. Materials Science and Engineering A 168, 235.

Hasmy, A., Anglaret, E., Foret, M., Pelous, J., Jullien, R., 1994. Small-angle neutron-scattering investigation of long-range correlations in silica aerogels: simulation and experiments. Physical Review B 50, 6006.

Hrubesh, L.W., 1998. Aerogel applications. Journal of Non-Crystalline Solids 225, 335.

Hughes, T.J.R., 1987. The Finite Element Method: Linear Static and Dynamic Finite Element Analysis. Prentice Hall, New Jersey.

Kolb, M., Botet, R., Jullien, R., 1983. Scaling of kinetically growing clusters. Physical Review Letter 51, 1123.

Ma, H.-S., Roberts, A.P., Prévost, J.-H., Jullien, R., Scherer, G.W., 2000. Mechanical structure–property relationship of aerogels. Journal of Non-Crystalline Solids 277, 127.

Ma, H.-S., Prévost, J.-H., Jullien, R., Scherer, G.W., 2001. Computer simulation of mechanical structure–property relationship of aerogels. Journal of Non-Crystalline Solids 285, 216.

Ma, H.-S., Jullien, R., Scherer, G.W., 2002. Dangling bond deflection model: growth of gel network with loop structure. Physical Review E 65, 041403.

Ma, H.-S., Scherer, G.W. Loop structure in gels: evolution and elasticity implications, in preparation.

Meakin, P., 1983. Formation of fractal clusters and networks by irreversible diffusion-limited aggregation. Physical Review Letter 51, 1119.

Pekala, R.W., 1991. A comparison of mechanical properties and scaling law relationships for silica aerogels and their organic counterparts. In: Materials Research Society Symposium Proceedings, vol. 207, p. 197.

Prévost, J.-H., 1983. Dynaflow®. Princeton University, Princeton (last updated: 2002).

Przemieniecki, J.S., 1985. Theory of Matrix Structural Analysis. Dover Publications, New York.

Scherer, G.W., 1992. Bending of gel beams: method for characterizing elastic properties and permeability. Journal of Non-Crystalline Solids 142, 18.

Scherer, G.W., Smith, D.M., Qiu, X., Anderson, J.M., 1995a. Compression of aerogels. Journal of Non-Crystalline Solids 186, 316.

Scherer, G.W., Smith, D.M., Stein, D., 1995b. Deformation of aerogels during characterization. Journal of Non-Crystalline Solids 186, 309.

Timoshenko, S.P., Goodier, J.N., 1970. Theory of Elasticity, third ed. McGraw-Hill, Singapore.

Vacher, R., Woignier, T., Pelous, J., Courtens, E., 1988. Structure and self-similarity in silica aerogels. Physical Review B 37, 6500.

Woignier, T., Phalippou, J., Vacher, R., 1989. Parameters affecting elastic properties of silica aerogels. Journal of Materials Research 4, 688.